Environmental Science & Technology

Article

pubs.acs.org/est

Contribution of Nitrated Phenols to Wood Burning Brown Carbon Light Absorption in Detling, United Kingdom during Winter Time

Claudia Mohr,[†] Felipe D. Lopez-Hilfiker,[†] Peter Zotter,[‡] André S. H. Prévôt,[‡] Lu Xu,[§] Nga L. Ng,[§] Scott C. Herndon,[∥] Leah R. Williams,[∥] Jonathan P. Franklin,[∥] Mark S. Zahniser,[∥] Douglas R. Worsnop,[∥,⊥] W. Berk Knighton,[#] Allison C. Aiken,[▽] Kyle J. Gorkowski,[▽,○] Manvendra K. Dubey,[▽] James D. Allan,[♦] and Joel A. Thornton*[,†]

[†]Department of Atmospheric Sciences, University of Washington, Seattle, Washington 98195, United States

[‡]Paul Scherrer Institute, Laboratory for Atmospheric Chemistry, Villigen 5232, Switzerland

[§]Georgia Institute of Technology, School of Earth and Atmospheric Sciences, Atlanta, Georgia 30332, United States

[∥]Aerodyne Research, Inc., Billerica, Massachusetts 01821, United States

[⊥]Department of Physics, University of Helsinki, Helsinki 00014, Finland

[#]Department of Chemistry and Biochemistry, Montana State University, Bozeman, Montana 59717, United States

[▽]Los Alamos National Laboratory, Earth and Environmental Sciences Division, Los Alamos, New Mexico 87545, United States

[○]Civil and Environmental Engineering, Carnegie Mellon University, Pittsburgh, Pennsylvania 15213, United States

[♦]National Centre for Atmospheric Science & School of Earth, Atmopspheric and Environmental Sciences, University of Manchester, Manchester M13 9PL, United Kingdom

Supporting Information

ABSTRACT: We show for the first time quantitative online measurements of five nitrated phenol (NP) compounds in ambient air (nitrophenol $C_6H_5NO_3$, methylnitrophenol $C_7H_7NO_3$, nitrocatechol $C_6H_5NO_4$, methylnitrocatechol $C_7H_7NO_4$, and dinitrophenol $C_6H_4N_2O_5$) measured with a micro-orifice volatilization impactor (MOVI) high-resolution chemical ionization mass spectrometer in Detling, United Kingdom during January–February, 2012. NPs absorb radiation in the near-ultraviolet (UV) range of the electromagnetic spectrum and thus are potential components of poorly characterized light-absorbing organic matter ("brown carbon") which can affect the climate and air quality. Total NP concentrations varied between less than 1 and 98 ng m^{-3}, with a mean value of 20 ng m^{-3}. We conclude that NPs measured in Detling have a significant contribution from biomass burning with an estimated emission factor of 0.2 ng (ppb CO)$^{-1}$. Particle light absorption measurements by a seven-wavelength aethalometer in the near-UV (370 nm) and literature values of molecular absorption cross sections are used to estimate the contribution of NP to wood burning brown carbon UV light absorption. We show that these five NPs are potentially important contributors to absorption at 370 nm measured by an aethalometer and account for 4 ± 2% of UV light absorption by brown carbon. They can thus affect atmospheric radiative transfer and photochemistry and with that climate and air quality.

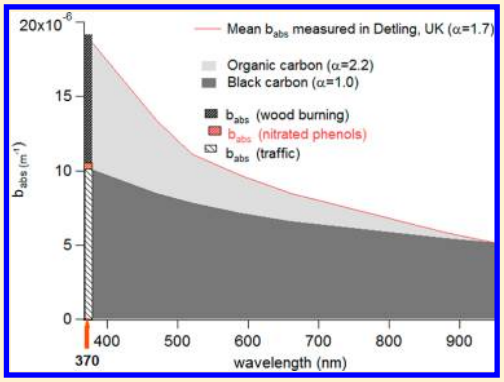

INTRODUCTION

Biomass burning is a major source of atmospheric carbonaceous aerosol. Globally, wildfires and biofuel combustion combined emitted an estimated 5 Tg/yr of black carbon (BC) and 10–50 Tg/yr of organic carbon (OC) in recent years.[1,2] Both BC and OC particulate matter (PM) affect human health[3] and climate.[4] BC is traditionally regarded as the most important light absorber in PM[5−7] given its high absorptivity per unit mass across the entire visible spectrum. In the near-ultraviolet (UV) range of the electromagnetic spectrum, OC can become an important light-absorber as well.[8−10] However, little is known about the sources and composition of light-absorbing organic matter, termed "brown carbon."[11] Brown carbon appears to be especially significant in biomass/biofuel combustion emissions,[12] yet specific light-absorbing compounds remain largely unidentified.[11,13]

Among the high number of poorly constrained brown carbon compounds are nitrated phenols (NPs). Absorption peak wavelengths of NPs such as nitrophenol (NPh, $C_6H_5NO_3$),

Received: February 13, 2013
Revised: May 14, 2013
Accepted: May 28, 2013
Published: May 28, 2013

methylnitrophenol (MNP, $C_7H_7NO_3$), nitrocatechol (NC, $C_6H_5NO_4$), methylnitrocatechol (MNC, $C_7H_7NO_4$), and dinitrophenol (DNP, $C_6H_4N_2O_5$) are between 292 and 351 nm, in the near-UV range of the electromagnetic spectrum, tailing off into the visible range.[14] In addition to a positive radiative forcing due to the absorption of visible radiation, aerosol extinction in the UV spectral region can further affect climate and air quality by reducing the solar actinic flux which drives atmospheric photochemistry and tropospheric ozone production in particular.[14,15] Moreover, NPs exert negative effects on ecosystem productivity[16] and human health.[17]

Sources of NP in the atmosphere include car exhaust and combustion processes of coal and wood,[18,19] with the latter being especially important: NPs were identified earlier as tracers for (mostly secondary) organic aerosol (OA) from biomass burning.[20−22] Semivolatile substituted phenols, the atmospheric oxidation of which is likely to form secondary OA, are among the most important compounds from the thermal degradation and pyrolysis of lignin, a vegetation structural material.[21,23,24] Emission factors of NP from biomass burning are in the range of 1 mg kg^{-1} of wood burned.[25]

NP can also be formed *in situ* by secondary chemistry. For example, NPs are formed in the gas phase by nitration of the reaction products of (methyl)phenols and OH or NO_3 in the presence of NO_x (NO + NO_2). Nitration of phenols also occurs in the condensed phase, suggesting a role for cloud or aerosol processing as a source.[18,26,27] In particular, the second nitration of NPh to DNP is thought to likely occur in the aqueous phase.[19] Phenols were reported to react in a biomass smoke plume with NO_x to form NPh within hours, thus influencing the production of ozone in aged smoke.[28,29] 2NP and 4NP are the prevalent isomers resulting from these reactions. In the atmosphere, the concentration of 4NP is often higher than that of 2NP in both the gas and liquid phases.[19,25] Atmospheric sinks include reactions with OH and NO_3 radicals, photolysis, condensed-phase processes, and wet deposition.[30] Off-line measurements of ambient concentrations of particulate NP range from a few up to tens of ng m^{-3}.[19,22,27,31]

Atmospheric NPs are commonly measured by first sampling ambient air through filters, often for hours up to days. Days or weeks later, the collected material is extracted and analyzed by GC/MS,[19,23] or more recently, HPLC/MS,[31] and HPLC/(-)ESI-MS.[20,27] Here, we show for the first time quantitative online measurements of NP measured with a micro-orifice volatilization impactor high-resolution chemical ionization mass spectrometer in Detling, United Kingdom during winter time. We use concurrent particle light absorption measurements by a seven-wavelength aethalometer and literature values of molecular absorption cross sections to estimate the contribution of NP to wood burning brown carbon UV light absorption.

METHODOLOGY

Field Site. Ambient measurements were conducted in Detling, United Kingdom, within the ClearfLo project (Clean Air for London, www.clearflo.ac.uk), to study boundary layer pollution across London, United Kingdom.[32] A multi-institution team deployed an extensive suite of in situ and remote sensing instrumentation to study the sources and evolution of aerosol downwind of London and the European Continent from January 10 through February 15, 2012 at the rural field site in Detling (51°18′ 6.952″ N, 0°35′22.178″ E). The Detling site is located ∼45 km southeast of London on a plateau (200 m asl), surrounded by fields and close to a permanent monitoring site operated by Maidstone Borough Council. Approximately 150 m south of the site is a busy road carrying ∼160 000 vehicles per day.[33] Villages and towns are all located in the plain. The English Channel is 50 km to the southeast and the North Sea is 25 km to the northeast. Surface wind direction varied over the campaign such that air was sampled from all of the above sectors, providing a useful contrast in source regions (Figure S1 in the Supporting Information, SI). The Detling site is a suitable location to study biomass burning emissions. Domestic burning, currently on the rise in the United Kingdom, is prevalent in the area[34] (SI, Figure S2a,b).

MOVI-HRToF-CIMS. NP data presented here were acquired with a micro-orifice volatilization impactor high-resolution time-of-flight chemical ionization mass spectrometer (MOVI-HRToF-CIMS, Aerodyne Research Inc., USA). With this instrument, both gas and particle phase organic species can be quantified on time scales of ≤1 s (gases) and >30 min (particle-phase compounds). A detailed description is provided elsewhere.[35,36] In brief, the MOVI inlet samples gas phase compounds while inertially impacting particles on a post (cut-point diameter d_{50}, aerodynamic diameter of 50% collection efficiency = 0.13 μm) and subsequently detects compounds on the impaction post via temperature programmed thermal desorption. Uncertainties related to the separation of gas and particle phase compounds inherent to the MOVI design are addressed below. Our focus here is on characterizing the first online detection of NPs to provide insights into their sources and possible contribution to light absorption measured by an aethalometer. Hence, we present data from thermal desorption measurements only.

Compared to the version described previously,[36] the MOVI used here employed a thermally isolated collection post actively temperature-controlled by water circulation, which allows the manifold body to be heated to ∼200 °C while the collection post is kept at ambient temperature during particle collection. The ion−molecule region (IMR) was conductively heated by the hot MOVI body to ∼70 °C. This approach improves the transfer of desorbed compounds to the mass spectrometer and increases the impaction measurement duty cycle.

NPs were detected via negative-ion chemical ionization (CI) in the IMR (∼68 Torr) using acetate ions ($CH_3C(O)O^-$) as the reagent.[37,38] Acetate ions abstract protons from compounds having higher gas-phase acidities than acetic acid, which includes most carboxylic acids, nitrophenols, and inorganic volatile acids, to form the corresponding anion of the conjugate base. While the instrument also periodically operated in positive ion mode, utilizing $H_3O^+(H_2O)_n$, only negative ion mode data will be shown here. After ionization, ions pass through the collisional dissociation chamber (CDC, ∼2.2 Torr) where tunable electric fields are used to break apart ion−molecule clusters[36,39] and which was operated under relatively strong declustering conditions (see SI). The resulting ions are mass analyzed and detected in a high-resolution time-of-flight mass spectrometer (TOFWERK AG, Switzerland; V-mode only, mass resolving power = 5000 for m/Q ≥ 250 Th, mass accuracy = ±20 ppm). Ion count rates were normalized to the sum of the reagent ion signal ($CH_3C(O)O^-$ and $CH_3C(O)$-$OH.CH_3C(O)O^-$). All data were analyzed using Matlab-based code written at the University of Washington and TofTools from the University of Helsinki.[40]

The MOVI-HRToF-CIMS was located inside a ventilated trailer and operated nearly continuously between January 27

Table 1. Nitrated Phenol Compounds Detected in Detling, Their Chemical Formulae, Tentative Structures, Sensitivities Based on Calibrations, The Mean Mass Concentrations Measured during the Field Campaign ±1 Standard Deviation, The Wave Lengths of Their Maximal Absorption, and Their Liquid Molecular Absorption Cross Sections Based on Ref 14[a]

Compound	m/Q detected, deproto-nated (Th)	Formula	Tentative structure (alternative structures are possible)	Sensitivity (counts ng^{-1})	mean conc. Detling ($ng\ m^{-3}$)	λ_{max} (nm)	Liquid molec. abs. cross section ($10^{17} cm^2\ molec^{-1}$)
Nitro-phenol (NPh)	138.019	$C_6H_5NO_3$	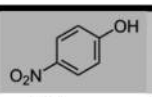	$1.6 \pm 0.2 \times 10^{7}$ (4)	0.02	317 (4)	3.63 (4)
Methyl-nitro-phenol (MNP)	152.035	$C_7H_7NO_3$	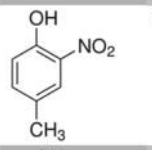	$4.0 \pm 0.1 \times 10^{4}$ (4,2)	5.0	319 (2,4)	3.44 (2,4)
Nitro-catechol (NC)	154.014	$C_6H_5NO_4$	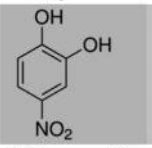	$2.6 \pm 0.3 \times 10^{4}$ (4)	2.5	337 (4)	4.10 (4)
Methyl-nitro-catechol (MNC)	168.030	$C_7H_7NO_4$	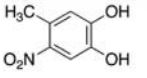	*4.0 ± 0.1 x 10⁴*	8.2	-	
Dinitro-phenol (DNP)	183.004	$C_6H_4N_2O_5$	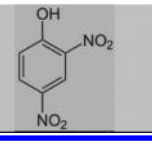	*4.0 ± 0.1 x 10⁴*	3.0	292 (2,4)	3.82 (2,4)

[a]The superscript *(4)* denotes values based on the 4-nitrophenol isomer; *(4,2)* stands for 4-methyl-2-nitrophenol, *(2,4)* for 2-methyl-4-nitrophenol/2,4-dinitrophenol. The numbers in italics are estimated, not measured.

and February 15, 2012. The sampling inlet consisted of 12 mm OD Teflon FEP tubing of 220 cm length. An impactor was mounted at the top of the inlet, 1 m above the container roof to remove particles >3 μm. In addition to sampling ambient air, instrumental background determinations in zero air added to the top of the inlet and sensitivity calibrations using additions of a formic acid standard to the ambient flow were routinely conducted throughout the campaign (for more details, see the SI). A typical measurement sequence was as follows (see Figure S3): For a given ion polarity mode, two ambient air sampling cycles were followed by a zero air sampling cycle. A cycle consisted of sampling either ambient or zero air at 10 L min^{-1} with simultaneous particle impaction for 10 min, followed by subsequent temperature programmed thermal desorption. During a desorption, the impaction post temperature was ramped from ~20 to 200 °C over 5 min, followed by a 10 min soak with both body and post at 200 °C. Approximately 2 min at the beginning and end of a desorption were required for transition to/from sampling modes. Thus, a measurement point reported here represents one 15 min integration.

Frequent additions of a formic acid standard (permeation tube, output 120 ng min^{-1} at 70 °C, KIN-TEK, USA) to the sampling inlet were made for assessing the robustness of inlet transfer, ionization, ion transmission, and detector efficiency. The instrumental sensitivity to formic acid was in the range of 10−15 Hz $pptv^{-1}$ (in negative ion mode) throughout the campaign. Systematic variability, driven presumably by swings in trailer and inlet temperature, dominated the variation in the formic acid calibration factors with adjacent point-to-point differences in sensitivity below 9%. Calibrations of compounds detected by desorption from the impaction post were performed in the laboratory before and after the campaign given the difficulty of accurately producing the very dilute standards while in the field.

Quantification of Nitrated Phenols. Table 1 gives an overview of the five NP compounds detected in Detling, their chemical formulas, tentative structures (alternative structures are possible), and detection sensitivity. The attribution of ion signals to NP is driven by the measured elemental composition and that the parent compound must have a gas-phase acidity that is higher than that of acetic acid. Thermal decomposition of larger compounds may be contributing to the signal we observe. Determination of the response factors for the NP was evaluated from calibration experiments in the laboratory after the campaign by injecting known quantities (in solution) into the MOVI. For further details, see the SI, Figure S4. The resulting sensitivities ranged from $(2.6-4.0 \pm 0.1) \times 10^4$ counts ng^{-1} for 4NC and 4M2NP, respectively, to $(1.6 \pm 0.2) \times 10^7$ counts ng^{-1} for 4NP. 2NP was not used for sensitivity calculations because 4NP is regarded as the more abundant isomer resulting from atmospheric processes.[19,25] For DNP and MNC, we assumed the same sensitivity (and thus also thermal decomposition rate) as measured for MNP, based on the similarity of the chemical structure of these compounds. The instrument sensitivity to 4M2NP and 4NC is comparable to the sensitivity to palmitic, azelaic, and trycarballylic acid ($1.1 \pm 0.02 \times 10^4$, $2.3 \pm 0.05 \times 10^4$, and $7.8 \pm 0.2 \times 10^4$ counts ng^{-1}, respectively) as measured by Yatavelli et al.[36] The very high sensitivity of our instrument to 4NP cannot be fully explained; however, order-of-magnitude differences between 4NP and

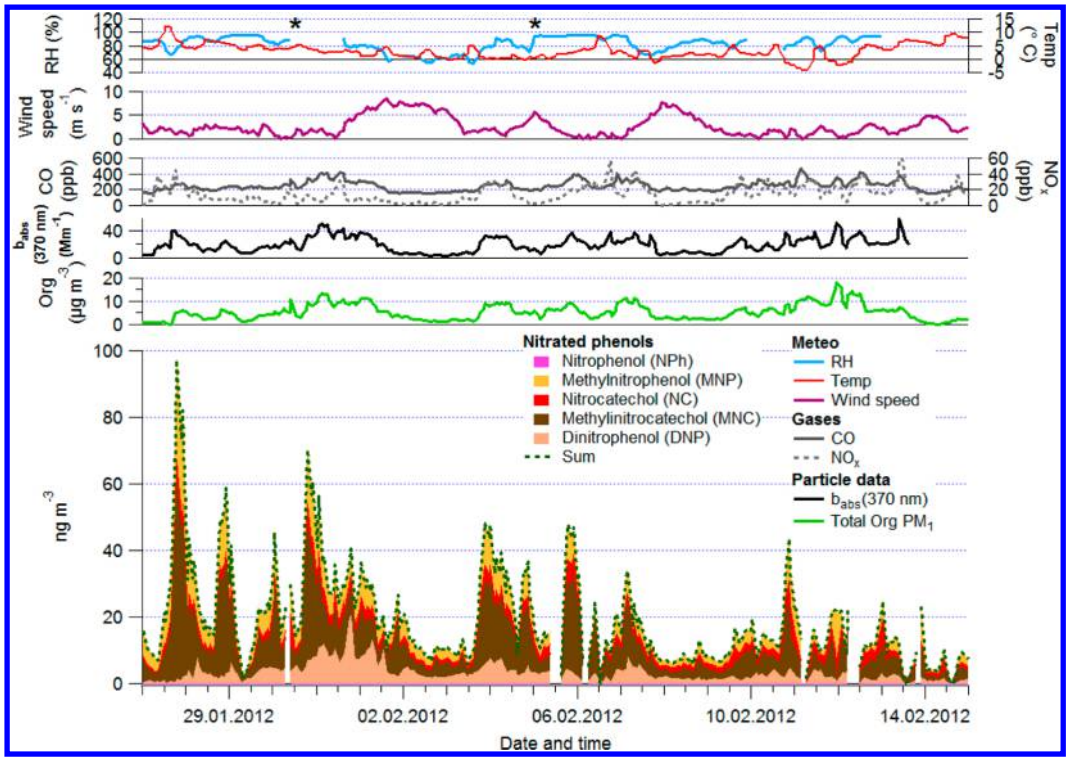

Figure 1. Time series of ambient temperature (Temp) and relative humidity (RH), NO_x, CO, the fraction of b_{abs} measured with an aethalometer at 370 nm (b_{abs}(370 nm)), total organic PM_1, and particulate nitrated phenols (stacked) as identified by the CIMS during the ClearfLo campaign in Detling. The asterisks denote snow fall incidents.

2NP sensitivities were also observed in electrospray ionization (ESI) mass spectrometry,[41] and we observed nearly the same relative differences in response between 4NP and the other compounds when sampling the vapor from the pure substances. Differences in gas-phase acidity between 4NP and 2NP (~36 kJ/mol[42]) likely cannot completely explain these differences; aromatic substituent effects of the nitro-group being ortho to the phenolic moiety may play a role.

NP signals reported here are the integrated desorption spectra corrected by corresponding interpolated adjacent blank cycle spectra. There are both positive and negative biases associated with the measurement approach which lead to uncertainties as summarized below:

- The background signals measured in zero air were at most 10% of the signal measured during an ambient cycle. Identification of ion elemental composition during a background was difficult due to the low signal, but the full signal within 20 ppm of the exact mass of the corresponding NP ion peak was subtracted, regardless.
- Particles bouncing off the post and hitting the hot MOVI body walls will evaporate and be counted as a gas phase signal. Yatavelli and Thornton[35] estimated a 35% loss of the desorption signal due to bounce for amorphous solid particles. Since the phase and bounce characteristics of the particles at Detling are unknown, we assume this value represents an upper limit for the bounce effect.
- Measurements of ambient aerosol size distributions at the top and at the bottom of the inlet prior to and during the campaign suggested a 56% particle mass transmission through the inlet for particles with a diameter above the MOVI cutpoint of 130 nm.
- Adsorption of gases to the impaction post during particle impaction can lead to a positive bias in the desorption signal. This effect likely depends on partitioning conditions such as temperature and mass loadings in the atmosphere and inside the MOVI. Tests done during the campaign were inconclusive but suggest an upper limit of 50% contribution for these compounds.
- Summing the uncertainties in quadrature of the first three negative biases yields 57%, which is close to the uncertainty of 50% of the positive gas phase adsorption effect. We therefore simply report a ±50% uncertainty in our measurements.

Particle Light Absorption. Particulate light absorption was derived during ClearfLo from an aethalometer, model AE 31 (Magee Scientific, USA). It measures the light attenuation b_{ATN} over a broad region of the visible spectrum of wavelengths (at λ = 370, 470, 520, 590, 660, 880, and 950 nm). b_{ATN} was corrected for multiple scattering of the light beam within the unloaded filter matrix (C = 3.095)[43] and for the "shadowing" caused by the deposited particles (f = 1.2) following the procedure of Weingartner et al.,[44] yielding the aerosol absorption coefficient b_{abs} (using an attenuation cross-section σ_{ATN} of 31.1, 28.1, 24.8, 22.2, 16.6, and 15.4 $m^2\ g^{-1}$ for the wavelengths 370−950 nm).

RESULTS AND DISCUSSION

Overview ClearfLo Campaign. The top five panels of Figure 1 show the time series of temperature, relative humidity (RH), wind speed, NO_X, CO, the light absorption coefficient (b_{abs}) measured at λ = 370 nm by the aethalometer, and total PM_1 organics measured by a high-resolution time-of-flight aerosol mass spectrometer (AMS, Aerodyne Research Inc., USA, collection efficiency = 0.5). The temporal patterns of all nonmeteorological measurements show a similar behavior, indicating that they are largely subject to common source regions and/or removal processes such as transport, dilution, or

dx.doi.org/10.1021/es400683v | Environ. Sci. Technol. 2013, 47, 6316−6324

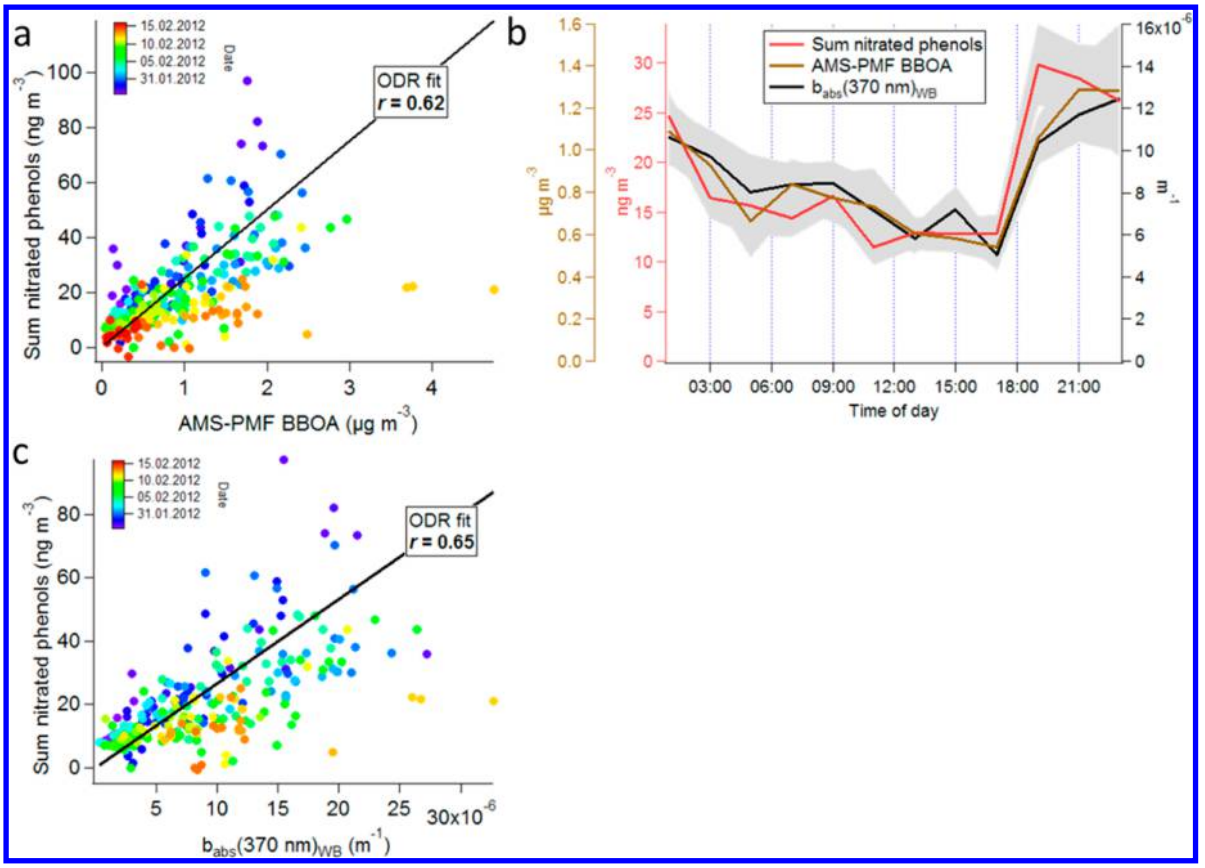

Figure 2. Scatterplot with the orthogonal distance regression (ODR) fit and the correlation coefficient *r* of the sum of NP identified in this study and (a) OA from biomass burning based on PMF analyses of AMS data (AMS-PMF BBOA) and (c) the fraction of b_{abs} measured with an aethalometer at 370 nm from wood burning ($b_{abs}(370\ nm)_{WB}$). Panel b shows the diurnal pattern of the time series of the sum of NAs, AMS-PMF BBOA, and $b_{abs}(370\ nm)_{WB}$. The shaded gray areas represent ± the standard error of the mean.

scavenging.[45] Temperatures were relatively low during the campaign, between −4 and 12 °C and often below 5 °C. High wind speeds around February 2nd and 9th led to periods with low concentrations of PM and gaseous species. Apart from the two episodes with high wind speeds from the northwest and the northeast, most days were dominated by relatively moderate wind speeds and thus influenced by local/regional emissions. The influence of London outflow was most important only at the end of January/beginning of February.

NO_X concentrations of up to 60 ppb are most likely due to the proximity of the site to a busy road (see a diurnal pattern in Figure S5). CO concentrations of 200 ppb and more were measured, and their diurnal pattern suggests influences from both traffic emissions and biomass burning for domestic heating purposes due to the presence of a morning peak that would be associated with the roadway and high concentrations in the evening hours as would be expected from domestic heating. Total OA reached values of up to 17 $\mu g\ m^{-3}$, with a mean of 5.2 $\mu g\ m^{-3}$, for the period when the MOVI-HRToF-CIMS was measuring, comparable to concentrations measured in urban areas or areas <100 miles downwind of major cities in the United Kingdom,[46] but lower than the values measured in downtown London in previous years.[47] The similarity of the time series of b_{abs} measured at 370 nm with total OA indicates a potential influence of organic compounds on particle light absorption measured at this wavelength.[8]

Nitrated Phenols. Figure 1 shows the stacked time series of the five NP compounds quantified by the MOVI-HRToF-CIMS: NPh, NC, MNP, MNC, and DNP. A representative mass spectrum is provided in the SI (Figure S6). The compound with the highest concentrations is generally MNC, followed by DNP and MNP. Total concentrations varied between less than 1 and 98 ng m^{-3}, with a mean value of 20 ng m^{-3}, contributing on average ∼0.5% of total OA measured by the AMS. These concentrations are comparable to the MNC mass concentrations measured in PM_{10} in rural Germany in winter time (up to 29 ng m^{-3});[27] yearly average PM_3 mass concentrations of 1.57 ng m^{-3}, 2.48 ng m^{-3}, and 6.4 ng m^{-3} for 2-NPh, 4-NPh, and 4-NC, respectively, measured in Mainz, Germany;[31] and NP measurements in winter/spring in Rome, Italy.[19] Hoffman et al.[25] and Kitanovski et al.[22] found the fraction of phenolic compounds in organic particles from biomass burning to be 1−2%. We find that on average NPs make up ∼1% of the organic mass detected by the MOVI-HRToF-CIMS and assuming formic acid sensitivity for all organics besides NP. While formic acid represents a reasonable surrogate, having a sensitivity similar to the average measured for a group of specific compounds, application of this sensitivity to the entire mass spectrum carries significant uncertainty. Nonetheless, the contribution of NP to total OA that we estimate is similar to the previous independent estimates.

In order to assess possible sources of the five NP compounds identified in this study, the time series of their sum was compared to the time series of the three factors resulting from positive matrix factorization (PMF[48,49]) of the AMS organic aerosol data. For a detailed discussion of the PMF solution, see

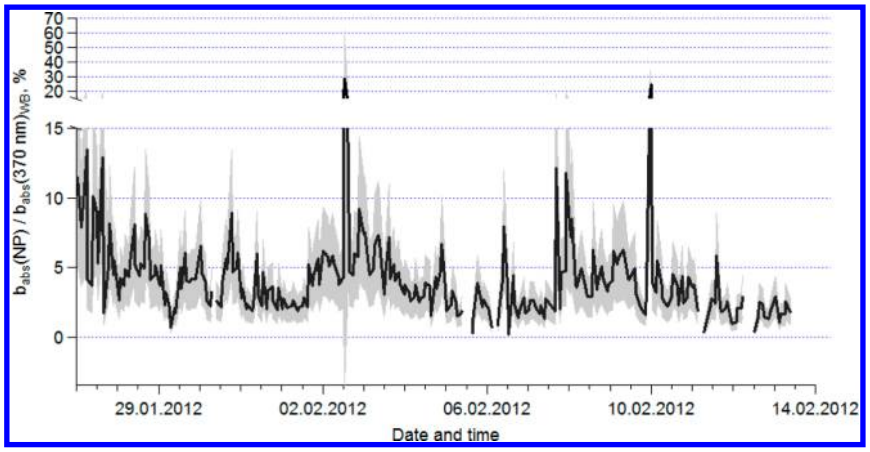

Figure 3. Time series of the percent ratio of the absorption from nitrated phenols (b_{abs}(NP)), based on literature value molecular absorption cross sections, to the total absorption measured by an aethalometer from wood burning carbonaceous matter at 370 nm ($b_{abs}(370\ nm)_{WB}$). The shaded areas denote the uncertainty in the ratio based on the $b_{abs}(370\ nm)_{WB}$ and b_{abs}(NP) signals: In addition to the 50% uncertainty of the MOVI-HRToF-CIMS data, measurement values of both time series were assigned a relative error between 0 (maximum values) and 100% (values closest to 0) and summed in quadrature.

the SI. The three factors identified were related to the following sources of organic aerosol: Hydrocarbon-like organic aerosol (HOA) from traffic emissions, oxygenated organic aerosol (OOA) related to secondary formation processes, and biomass burning organic aerosol (BBOA) related to solid fuel combustion for domestic heating purposes and open agricultural fires.[50] The highest correlation coefficient ($r(293) = 0.62$, $p < 0.05$, where 293 refers to the number of data points) was achieved when correlating the sum of the NP with BBOA (Figure 2a). This value was statistically different at the 95% confidence level from $r(293) = 0.34$, $p < 0.05$ for OOA and $r(293) = 0.35$, $p < 0.05$ for HOA. Correlation coefficients of the individual compounds with the PMF-AMS factors are presented in the SI (Table S2). The correlation of the sum of the NP with the time series of acetonitrile, a marker compound in biomass plumes,[51] measured by proton transfer reaction mass spectrometry (PTR-MS, Ionicon Analytik GmbH, Austria) using a calibrated response factor[52] yielded an $r(241)$ of 0.56, $p < 0.05$.

We conclude from the above that NPs measured in Detling have a significant contribution from biomass burning, in accordance with findings from other studies.[20,21] The campaign average diurnal pattern of both BBOA and the sum of NP (Figure 2b) supports the identification of solid fuel combustion for domestic heating purposes as a major source of NP. NP concentrations are highest in the evening and night when people are at home and likely heating. This finding is comparable to the diurnal pattern of BBOA measured in Zurich, Switzerland, and London and Machester, United Kingdom during winter.[45,53] In addition, the MOVI-HRToF-CIMS was used in Seattle during a few days of August 2011 when the area was severely impacted by nearby wildfires and a strong stagnation event. We detected all five compounds above background and at similar order of magnitude concentrations, though diurnal patterns were significantly different between the two data sets as might be expected given the controlled fuel burning in Detling and the wildfire source in Seattle.

NPs have been related to both primary biomass burning emissions and secondary processing of those emissions.[18,26−28,31] With the data at hand from both MOVI-HRToF-CIMS and the AMS, we cannot conclusively assign quantitative fractions of NP to either primary emissions or secondary formation processes. The time scales of the formation of secondary species in biomass burning plumes are on the order of several minutes to hours,[29,54] enough time for these compounds to reach the Detling measurements site after their precursors have been emitted in nearby towns and villages and insufficient time for these air masses to be processed such that they would have the same mass spectral pattern and temporal evolution as the more regional and more aged OOA compounds. Interestingly, the diurnal pattern of the signal we attribute to DNP shows a slightly different trend than the other four compounds with slightly increased concentrations in the afternoon and decreased concentrations in the evening/night compared to the other NPs (Figure S8). DNP is unique among the studied compounds as it is the only one that contains two nitro functional groups, suggesting that secondary photochemical or multiphase processes[18,19] may also be important for explaining its time evolution.

We can use the NPs measured in Detling and their relationship with CO to estimate an NP emission factor from biomass burning (including both primary and secondary NP). For this purpose, we select data when the ratio of BBOA to total OA was above 0.3 (the 90th percentile) and then regress the sum of NPs on the above-background CO mixing ratio ($\Delta CO = CO_{plume} - CO_{background}$). We determine $CO_{background}$ to be 100 ppb for this data set based on the x-axis intercept of the (HOA + BBOA) to CO regression analysis[55,56] (Figure S7). We then find an NP/CO emission ratio of 0.2 ng (ppb CO)$^{-1}$ for biomass burning influenced periods. Assuming an emission factor of 100 g of CO per kg of dry wood burned (value rounded from refs 57 and 58) yields an NP emission factor of ~15 mg kg^{-1} dry wood burned, which is an order of magnitude higher than the values reported by Hoffmann et al.[25] Note, however, that there is a wide range of CO emission factors reported and that we are not able to fully separate biomass burning from other NP sources in Detling. However, controlled burn experiments[59] using our methodology could provide more accurate emission estimates per biomass burned.

Light Absorption of NP. The NPs measured here have been shown to absorb in the near-UV range of the electromagnetic spectrum;[14] their maximum absorption wavelengths are shown in Table 1. The closest wavelength measured in the aethalometer is 370 nm. We chose to use aethalometer

data due to the proximity of the instrument's lowest wavelength to the NP maximum absorption wavelengths. Figure 2c shows a scatterplot of the sum of nitrated phenols and the light absorption coefficient at 370 nm for pure wood burning (WB) conditions ($b_{abs}(370\ nm)_{WB}$) derived from the aethalometer data. $b_{abs}(370\ nm)_{WB}$ was calculated using the aethalometer model developed by Sandradewi et al.,[60] based on the power law relationship between b_{abs} measured by the aethalometer and wavelength λ:

$$b_{abs} = k^{*}\lambda^{-\alpha} \quad (1)$$

k denotes a proportionality constant and α the Angström exponent. Further details can be found in the SI. The b_{abs} due to BC (carbon implied to have optical properties and composition similar to soot[11]) was calculated assuming α = 1[15,61,62] and subtracted from b_{abs}, yielding the absorption due to organic matter other than soot carbon (i.e., brown carbon).[12] Brown carbon accounts for up to 46% of the total absorption at 370 nm decreasing to <30% of the absorption at 520 nm (see SI, Figure S9). The fit to the brown carbon fraction yielded an Angström exponent of 2.2, which was used to calculate $b_{abs}(370\ nm)_{WB}$ (Formula S1 in the SI). $b_{abs}(370\ nm)_{WB}$ makes up 46% of the total absorption at 370 nm. We thus assume that (a) $b_{abs}(370\ nm)_{WB}$ consists entirely of brown carbon and that (b) brown carbon absorption in Detling is due to WB emissions. An $r(267)$ of 0.65, $p < 0.05$ and the diurnal pattern of $b_{abs}(370\ nm)_{WB}$ (Figure 2b) support a relationship between BBOA, light-absorbing NP, and particle light absorption measured in Detling. At Detling, there were multiple aerosol light absorption instruments, which showed generally good agreement (Figure S10). Zhang et al.[63] also found high correlation coefficients of NP in secondary OA and b_{abs} at 365 nm in Pasadena, California; though, in contrast to our analysis, they attributed the OA mainly to fossil carbon.

To assess the potential contribution of nitrated phenols to the light absorption at 370 nm due to WB brown carbon, we used the mass concentrations measured by the MOVI-HRToF-CIMS and mass absorption coefficients of the NP calculated based on literature values of the liquid-phase molecular absorption cross sections (see Table 1). Figure 3 shows the corresponding fraction of the absorption of WB brown carbon measured at 370 nm due to NP, which varies between below 1 and 29%, with a mean value 4 ± 2% (uncertainty range based on uncertainty in MOVI-HRToF-CIMS signal and outliers in the ratio due to low values of $b_{abs}(370\ nm)_{WB}$ and $b_{abs}(NP)$).

These first quantitative online measurements of five nitrophenols in ambient air in Detling, United Kingdom show that NPs may make up a small fraction of total OA in Detling (~0.5%) but are a potentially important contributor to light absorption in the near-UV by brown carbon from wood burning with implications for the anthropogenic impact on radiative transfer in this spectral region. These measurements and our knowledge of the associated measurement artifacts place important and useful constraints on the potential radiative impact of NP. Thus, while these results provide complementary support for measurements and analyses made by offline filter based techniques, reducing the uncertainty in these constraints further represents a continuing technological challenge to both the filter-based light absorption and chemical composition methods.

■ ASSOCIATED CONTENT

Supporting Information

ClearfLo field site, Detling, U. K., declustering conditions, measurement cycles during ClearfLo and gas phase calibrations, quantifications of nitrated phenols, ClearfLo mean diurnal pattern of NO_x and CO, positive matrix factorization (PMF), MOVI-HRToF-CIMS mass spectrum, correlation coefficient of individual NA compounds and AMS-PMF factors, CO background determination, diurnal pattern of dinitrophenol/nitrophenol, separation of b_{abs} into OC/BC and wood burning/traffic fractions, comparison of absorption measured by the aethalometer and PASS-3. This information is available free of charge via the Internet at http://pubs.acs.org.

■ AUTHOR INFORMATION

Corresponding Author

*Phone: +1 206-543-4010. E-mail: thornton@atmos.uw.edu.

Notes

The authors declare no competing financial interest.

■ ACKNOWLEDGMENTS

This work was supported by DOE-ASR GVAX grant DE-SC0006036, the NERC Clean Air For London (CLEARFLO) project [grant ref: NE/H00324X/1], and the National Centre for Atmospheric Science (NCAS). We thank David Green (King's College London), Carl Percival (University of Manchester), Christine Braban (Centre for Ecology and Hydrology), and the staff at the Kent Showground for their support during the campaign.

■ REFERENCES

(1) Chin, M.; Diehl, T.; Ginoux, P.; Malm, W. Intercontinental transport of pollution and dust aerosols: implications for regional air quality. *Atmos. Chem. Phys.* **2007**, *7* (21), 5501−5517, DOI: 10.5194/acp-7-5501-2007.

(2) Vermote, E.; Ellicott, E.; Dubovik, O.; Lapyonok, T.; Chin, M.; Giglio, L.; Roberts, G. J. An approach to estimate global biomass burning emissions of organic and black carbon from MODIS fire radiative power. *J. Geophys. Res.* **2009**, *114* (D18), D18205 DOI: 10.1029/2008jd011188.

(3) Nel, A. Air pollution-related illness: Effects of particles. *Science* **2005**, *308* (5723), 804−806, DOI: 10.1126/science.1108752.

(4) *IPCC Fourth Assessment Report: The Physical Science Basis, Working Group I, Final Report*; IPCC: Geneva, Switzerland, 2007. Available at http://www.ipcc.ch/ipccreports/ar4-wg1.htm.

(5) Hansen, A. D. A.; Rosen, H.; Novakov, T. The Aethalometer - an Instrument for the Real-Time Measurement of Optical-Absorption by Aerosol-Particles. *Sci. Total Environ.* **1984**, *36* (Jun), 191−196, DOI: 10.1016/0048-9697(84)90265-1.

(6) Penner, J. E.; Eddleman, H.; Novakov, T. Towards the Development of a Global Inventory for Black Carbon Emissions. *Atmos. Environ.* **1993**, *27* (8), 1277−1295, DOI: 10.1016/0960-1686(93)90255-W.

(7) Ramanathan, V.; Carmichael, G. Global and regional climate changes due to black carbon. *Nat. Geosci.* **2008**, *1* (4), 221−227, DOI: 10.1038/Ngeo156.

(8) Yang, M.; Howell, S. G.; Zhuang, J.; Huebert, B. J. Attribution of aerosol light absorption to black carbon, brown carbon, and dust in China - interpretations of atmospheric measurements during EAST-AIRE. *Atmos. Chem. Phys.* **2009**, *9* (6), 2035−2050, DOI: 10.5194/acp-9-2035-2009.

(9) Bahadur, R.; Praveen, P. S.; Xu, Y. Ramanathan. Solar absorption by elemental and brown carbon determined from spectral observations. *Proc. Natl. Acad. Sci.* **2012**, 1−14, DOI: 10.1073/pnas.1205910109.

(10) Flowers, B. A.; Dubey, M. K.; Mazzoleni, C.; Stone, E. A.; Schauer, J. J.; Kim, S.; Yoon, S. C. Optical-chemical-microphysical relationships and closure studies for mixed carbonaceous aerosols observed at Jeju Island; 3-laser photoacoustic spectrometer, particle sizing, and filter analysis. *Atmos. Chem. Phys.* **2010**, *10* (21), 10387−10398, DOI: 10.5194/acp-10-10387-2010.
(11) Andreae, M. O.; Gelencser, A. Black carbon or brown carbon? The nature of light-absorbing carbonaceous aerosols. *Atmos. Chem. Phys.* **2006**, *6*, 3131−3148, DOI: 10.5194/acp-6-3131-2006.
(12) Kirchstetter, T. W.; Thatcher, T. L. Contribution of organic carbon to wood smoke particulate matter absorption of solar radiation. *Atmos. Chem. Phys.* **2012**, *12* (14), 6067−6072, DOI: 10.5194/acp-12-6067-2012.
(13) Moosmuller, H.; Chakrabarty, R. K.; Arnott, W. P. Aerosol light absorption and its measurement: A review. *J. Quant. Spectrosc. Radiat. Transfer* **2009**, *110* (11), 844−878, DOI: 10.1016/j.jqsrt.2009.02.035.
(14) Jacobson, M. Z. Isolating nitrated and aromatic aerosols and nitrated aromatic gases as sources of ultraviolet light absorption. *J. Geophys. Res.: Atmos.* **1999**, *104* (D3), 3527−3542, DOI: 10.1029/1998jd100054.
(15) Kirchstetter, T. W.; Novakov, T.; Hobbs, P. V. Evidence that the spectral dependence of light absorption by aerosols is affected by organic carbon. *J. Geophys. Res.: Atmos.* **2004**, *109* (D21), DOI 10.1029/2004jd004999.
(16) Grosjean, D. Atmospheric Chemistry of Toxic Contaminants 0.1. Reaction-Rates and Atmospheric Persistence. *J. Air Waste Manage.* **1990**, *40* (10), 1397−1402, DOI: 10.1080/10473289.1990.10466792.
(17) Huang, Q. G.; Wang, L. S.; Han, S. K. The Genotoxicity of Substituted Nitrobenzenes and the Quantitative Structure-Activity Relationship Studies. *Chemosphere* **1995**, *30* (5), 915−923, DOI: 10.1016/0045-6535(94)00450-9.
(18) Harrison, M.; Barra, S.; Borghesi, D.; Vione, D.; Arsene, C.; Iulianolariu, R. Nitrated phenols in the atmosphere: a review. *Atmos. Environ.* **2005**, *39* (2), 231−248, DOI: 10.1016/j.atmosenv.2004.09.044.
(19) Cecinato, A.; Di Palo, V.; Palo, V.; Pomata, D.; Tomasi Scianò, M. C.; Possanzini, M. Measurement of phase-distributed nitrophenols in Rome ambient air. *Chemosphere* **2005**, *59* (5), 679−683, DOI: 10.1016/j.chemosphere.2004.10.045.
(20) Kitanovski, Z.; Grgic, I.; Yasmeen, F.; Claeys, M.; Cusak, A. Development of a liquid chromatographic method based on ultraviolet-visible and electrospray ionization mass spectrometric detection for the identification of nitrocatechols and related tracers in biomass burning atmospheric organic aerosol. *Rapid Commun. Mass Spectrom.* **2012**, *26* (7), 793−804, DOI: 10.1002/Rcm.6170.
(21) Schauer, J. J.; Kleeman, M. J.; Cass, G. R.; Simoneit, B. R. T. Measurement of emissions from air pollution sources. 3. C-1-C-29 organic compounds from fireplace combustion of wood. *Environ. Sci. Technol.* **2001**, *35* (9), 1716−1728, DOI: 10.1021/Es001331e.
(22) Kitanovski, Z.; Grgić, I.; Vermeylen, R.; Claeys, M.; Maenhaut, W. Liquid chromatography tandem mass spectrometry method for characterization of monoaromatic nitro-compounds in atmospheric particulate matter. *J. Chromatogr., A* **2012**, DOI: 10.1016/j.chroma.2012.10.021.
(23) Iinuma, Y.; Bruggemann, E.; Gnauk, T.; Muller, K.; Andreae, M. O.; Helas, G.; Parmar, R.; Herrmann, H. Source characterization of biomass burning particles: The combustion of selected European conifers, African hardwood, savanna grass, and German and Indonesian peat. *J. Geophys. Res-Atmos.* **2007**, *112* (D8), DOI 10.1029/2006jd007120.
(24) Simoneit, B. R. T. Biomass burning - A review of organic tracers for smoke from incomplete combustion. *Appl. Geochem.* **2002**, *17* (3), 129−162, DOI: 10.1016/S0883-2927(01)00061-0.
(25) Hoffmann, D.; Iinuma, Y.; Herrmann, H. Development of a method for fast analysis of phenolic molecular markers in biomass burning particles using high performance liquid chromatography/atmospheric pressure chemical ionisation mass spectrometry. *J. Chromatogr., A* **2007**, *1143* (1−2), 168−175, DOI: 10.1016/j.chroma.2007.01.035.
(26) Grosjean, D. Reactions of O-Cresol and Nitrocresol with Nox in Sunlight and with Ozone Nitrogen-Dioxide Mixtures in the Dark. *Environ. Sci. Technol.* **1985**, *19* (10), 968−974, DOI: 10.1021/Es00140a014.
(27) Iinuma, Y.; Böge, O.; Gräfe, R.; Herrmann, H. Methyl-Nitrocatechols: Atmospheric Tracer Compounds for Biomass Burning Secondary Organic Aerosols. *Environ. Sci. Technol.* **2010**, *44* (22), 8453−8459, DOI: 10.1021/es102938a.
(28) Bertschi, I.; Yokelson, R. J.; Ward, D. E.; Babbitt, R. E.; Susott, R. A.; Goode, J. G.; Hao, W. M. Trace gas and particle emissions from fires in large diameter and belowground biomass fuels. *J. Geophys. Res.* **2003**, *108* (D13), DOI 10.1029/2002JD002100.
(29) Mason, S. A.; Field, R. J.; Yokelson, R. J.; Kochivar, M. A.; Tinsley, M. R.; Ward, D. E.; Hao, W. M. Complex effects arising in smoke plume simulations due to inclusion of direct emissions of oxygenated organic species from biomass combustion. *J. Geophys. Res.: Atmos.* **2001**, *106* (D12), 12527−12539, DOI: 10.1029/2001jd900003.
(30) Northway, M. J.; Jayne, J. T.; Toohey, D. W.; Canagaratna, M. R.; Trimborn, A.; Akiyama, K. I.; Shimono, A.; Jimenez, J. L.; DeCarlo, P. F.; Wilson, K. R.; Worsnop, D. R. Demonstration of a VUV lamp photoionization source for improved organic speciation in an aerosol mass spectrometer. *Aerosol. Sci. Technol.* **2007**, *41* (9), 828−839, DOI: 10.1080/02786820701496587.
(31) Zhang, Y. Y.; Müller, L.; Winterhalter, R.; Moortgat, G. K.; Hoffmann, T.; Pöschl, U. Seasonal cycle and temperature dependence of pinene oxidation products, dicarboxylic acids and nitrophenols in fine and coarse air particulate matter. *Atmos. Chem. Phys.* **2010**, *10* (16), 7859−7873, DOI: 10.5194/acp-10-7859-2010.
(32) Bohnenstengel, S. ClearfLo Consortium. The ClearfLo project − understanding London's meteorology and composition. *Bull. Am. Meteorol. Soc.* **2013**, in preparation.
(33) Department for Transport Traffic counts. http://www.dft.gov.uk/traffic-counts/cp.php (Oct. 30, 2012).
(34) Department for Environment, F., and Rural Affairs National Atmospheric Emissions Inventory. naei.defra.gov.uk (February 9, 2013).
(35) Yatavelli, R. L. N.; Thornton, J. A. Particulate Organic Matter Detection Using a Micro-Orifice Volatilization Impactor Coupled to a Chemical Ionization Mass Spectrometer (MOVI-CIMS). *Aerosol. Sci. Technol.* **2010**, *44* (1), 61−74, DOI: 10.1080/02786820903380233.
(36) Yatavelli, R. L. N.; Lopez-Hilfiker, F.; Wargo, J. D.; Kimmel, J. R.; Cubison, M. J.; Bertram, T. H.; Jimenez, J. L.; Gonin, M.; Worsnop, D. R.; Thornton, J. A. A Chemical Ionization High-Resolution Time-of-Flight Mass Spectrometer Coupled to a Micro Orifice Volatilization Impactor (MOVI-HRToF-CIMS) for Analysis of Gas and Particle-Phase Organic Species. *Aerosol. Sci. Technol.* **2012**, *46* (12), 1313−1327, DOI: 10.1080/02786826.2012.712236.
(37) Veres, P.; Roberts, J. M.; Warneke, C.; Welsh-Bon, D.; Zahniser, M.; Herndon, S.; Fall, R.; de Gouw, J. Development of negative-ion proton-transfer chemical-ionization mass spectrometry (NI-PT-CIMS) for the measurement of gas-phase organic acids in the atmosphere. *Int. J. Mass Spectrom.* **2008**, *274* (1−3), 48−55, DOI: 10.1016/j.ijms.2008.04.032.
(38) Veres, P.; Roberts, J. M.; Burling, I. R.; Warneke, C.; de Gouw, J.; Yokelson, R. J. Measurements of gas-phase inorganic and organic acids from biomass fires by negative-ion proton-transfer chemical-ionization mass spectrometry. *J. Geophys. Res.: Atmos.* **2010**, *115*, DOI 10.1029/2010jd014033.
(39) Bertram, T. H.; Kimmel, J. R.; Crisp, T. A.; Ryder, O. S.; Yatavelli, R. L. N.; Thornton, J. A.; Cubison, M. J.; Gonin, M.; Worsnop, D. R. A field-deployable, chemical ionization time-of-flight mass spectrometer. *Atmos. Meas. Tech.* **2011**, *4* (7), 1471−1479, DOI: 10.5194/amt-4-1471-2011.
(40) Junninen, H.; Ehn, M.; Petäjä, T.; Luosujärvi, L.; Kotiaho, T.; Kostiainen, R.; Rohner, U.; Gonin, M.; Fuhrer, K.; Kulmala, M.; Worsnop, D. R. A high-resolution mass spectrometer to measure atmospheric ion composition. *Atmos. Meas. Tech.* **2010**, *3* (4), 1039−1053, DOI: 10.5194/amt-3-1039-2010.

(41) Desyater, Y. Personal communication, 2012.
(42) *NIST Chemistry WebBook*, April 17, 2013 ed.; U.S. Secretary of Commerce: Washington, DC, 2013.
(43) Collaud Coen, M.; Weingartner, E.; Apituley, A.; Ceburnis, D.; Fierz-Schmidhauser, R.; Flentje, H.; Henzing, J. S.; Jennings, S. G.; Moerman, M.; Petzold, A.; Schmid, O.; Baltensperger, U. Minimizing light absorption measurement artifacts of the aethalometer: evaluation of five correction algorithms. *Atmos. Meas. Tech.* **2010**, *3* (2), 457−474, DOI: 10.5194/amt-3-457-2010, 2010.
(44) Weingartner, E.; Saathoff, H.; Schnaiter, M.; Streit, N.; Bitnar, B.; Baltensperger, U. Absorption of light by soot particles: determination of the absorption coefficient by means of aethalometers. *J. Aerosol. Sci.* **2003**, *34* (10), 1445−1463, DOI: 10.1016/S0021-8502(03)00359-8.
(45) Lanz, V. A.; Alfarra, M. R.; Baltensperger, U.; Buchmann, B.; Hueglin, C.; Szidat, S.; Wehrli, M. N.; Wacker, L.; Weimer, S.; Caseiro, A.; Puxbaum, H.; Prevot, A. S. H. Source attribution of submicron organic aerosols during wintertime inversions by advanced factor analysis of aerosol mass spectra. *Environ. Sci. Technol.* **2008**, *42* (1), 214−220, DOI: 10.1021/Es0707207.
(46) Zhang, Q.; Jimenez, J. L.; Canagaratna, M. R.; Allan, J. D.; Coe, H.; Ulbrich, I.; Alfarra, M. R.; Takami, A.; Middlebrook, A. M.; Sun, Y. L.; Dzepina, K.; Dunlea, E.; Docherty, K.; DeCarlo, P. F.; Salcedo, D.; Onasch, T.; Jayne, J. T.; Miyoshi, T.; Shimono, A.; Hatakeyama, S.; Takegawa, N.; Kondo, Y.; Schneider, J.; Drewnick, F.; Borrmann, S.; Weimer, S.; Demerjian, K.; Williams, P.; Bower, K.; Bahreini, R.; Cottrell, L.; Griffin, R. J.; Rautiainen, J.; Sun, J. Y.; Zhang, Y. M.; Worsnop, D. R. Ubiquity and dominance of oxygenated species in organic aerosols in anthropogenically-influenced Northern Hemisphere midlatitudes. *Geophys. Res. Lett.* **2007**, *34* (13), L13801 DOI: 10.1029/2007GL029979.
(47) Harrison, R. M.; Dall'Osto, M.; Beddows, D. C. S.; Thorpe, A. J.; Bloss, W. J.; Allan, J. D.; Coe, H.; Dorsey, J. R.; Gallagher, M.; Martin, C.; Whitehead, J.; Williams, P. I.; Jones, R. L.; Langridge, J. M.; Benton, A. K.; Ball, S. M.; Langford, B.; Hewitt, C. N.; Davison, B.; Martin, D.; Petersson, K. F.; Henshaw, S. J.; White, I. R.; Shallcross, D. E.; Barlow, J. F.; Dunbar, T.; Davies, F.; Nemitz, E.; Phillips, G. J.; Helfter, C.; Di Marco, C. F.; Smith, S. Atmospheric chemistry and physics in the atmosphere of a developed megacity (London): an overview of the REPARTEE experiment and its conclusions. *Atmos. Chem. Phys.* **2012**, *12* (6), 3065−3114, DOI: 10.5194/acp-12-3065-2012.
(48) Paatero, P.; Tapper, U. Analysis of different modes of factor-analysis as least-squares fit problems. *Chemom. Intell. Lab. Syst.* **1993**, *18* (2), 183−194, DOI: 10.1016/0169-7439(93)80055-M.
(49) Paatero, P.; Tapper, U. Positive matrix factorization - a nonnegative factor model with optimal utilization of error-estimates of data values. *Environmetrics* **1994**, *5* (2), 111−126, DOI: 10.1002/env.3170050203.
(50) Ulbrich, I. M.; Canagaratna, M. R.; Zhang, Q.; Worsnop, D. R.; Jimenez, J. L. Interpretation of organic components from positive matrix factorization of aerosol mass spectrometric data. *Atmos. Chem. Phys.* **2009**, *9* (9), 2891−2918, DOI: 10.5194/acp-9-2891-2009.
(51) Holzinger, R.; Williams, J.; Salisbury, G.; Klupfel, T.; deReus, M.; Traub, M.; Crutzen, P. J.; Lelieveld, J. Oxygenated compounds in aged biomass burning plumes over the Eastern Mediterranean: evidence for strong secondary production of methanol and acetone. *Atmos. Chem. Phys.* **2005**, *5*, 39−46, DOI: 10.5194/acp-5-39-2005.
(52) Rogers, T. M.; Grimsrud, E. P.; Herndon, S. C.; Jayne, J. T.; Kolb, C. E.; Allwine, E.; Westberg, H.; Lamb, B. K.; Zavala, M.; Molina, L. T.; Molina, M. J.; Knighton, W. B. On-road measurements of volatile organic compounds in the Mexico City metropolitan area using proton transfer reaction mass spectrometry. *Int. J. Mass Spectrom.* **2006**, *252* (1), 26−37, DOI: 10.1016/j.ijms.2006.01.027.
(53) Allan, J. D.; Williams, P. I.; Morgan, W. T.; Martin, C. L.; Flynn, M. J.; Lee, J.; Nemitz, E.; Phillips, G. J.; Gallagher, M. W.; Coe, H. Contributions from transport, solid fuel burning and cooking to primary organic aerosols in two UK cities. *Atmos. Chem. Phys.* **2010**, *10* (2), 647−668.
(54) Heringa, M. F.; DeCarlo, P. F.; Chirico, R.; Tritscher, T.; Dommen, J.; Weingartner, E.; Richter, R.; Wehrle, G.; Prevot, A. S. H.; Baltensperger, U. Investigations of primary and secondary particulate matter of different wood combustion appliances with a high-resolution time-of-flight aerosol mass spectrometer. *Atmos. Chem. Phys.* **2011**, *11* (12), 5945−5957, DOI: 10.5194/acp-11-5945-2011.
(55) DeCarlo, P. F.; Dunlea, E. J.; Kimmel, J. R.; Aiken, A. C.; Sueper, D.; Crounse, J.; Wennberg, P. O.; Emmons, L.; Shinozuka, Y.; Clarke, A.; Zhou, J.; Tomlinson, J.; Collins, D. R.; Knapp, D.; Weinheimer, A. J.; Montzka, D. D.; Campos, T.; Jimenez, J. L. Fast airborne aerosol size and chemistry measurements above Mexico City and Central Mexico during the MILAGRO campaign. *Atmos. Chem. Phys.* **2008**, *8* (14), 4027−4048, DOI: 10.5194/acp-8-4027-2008.
(56) de Gouw, J. A.; Welsh-Bon, D.; Warneke, C.; Kuster, W. C.; Alexander, L.; Baker, A. K.; Beyersdorf, A. J.; Blake, D. R.; Canagaratna, M.; Celada, A. T.; Huey, L. G.; Junkermann, W.; Onasch, T. B.; Salcido, A.; Sjostedt, S. J.; Sullivan, A. P.; Tanner, D. J.; Vargas, O.; Weber, R. J.; Worsnop, D. R.; Yu, X. Y.; Zaveri, R. Emission and chemistry of organic carbon in the gas and aerosol phase at a sub-urban site near Mexico City in March 2006 during the MILAGRO study. *Atmos. Chem. Phys.* **2009**, *9* (10), 3425−3442, DOI: 10.5194/acp-9-3425-2009.
(57) Andreae, M. O.; Merlet, P. Emission of trace gases and aerosols from biomass burning. *Global Biogeochem. Cycles* **2001**, *15* (4), 955−966, DOI: 10.1029/2000GB001382.
(58) McDonald, J. D.; Zielinska, B.; Fujita, E. M.; Sagebiel, J. C.; Chow, J. C.; Watson, J. G. Fine particle and gaseous emission rates from residential wood combustion. *Environ. Sci. Technol.* **2000**, *34* (11), 2080−2091, DOI: 10.1021/Es9909632.
(59) Levin, E. J. T.; McMeeking, G. R.; Carrico, C. M.; Mack, L. E.; Kreidenweis, S. M.; Wold, C. E.; Moosmüller, H.; Arnott, W. P.; Hao, W. M.; Collett, J. L.; Malm, W. C. Biomass burning smoke aerosol properties measured during Fire Laboratory at Missoula Experiments (FLAME). *J. Geophys. Res,: Atmos.* **2010**, *115* (D18), DOI 10.1029/2009jd013601.
(60) Sandradewi, J.; Prevot, A. S. H.; Szidat, S.; Perron, N.; Alfarra, M. R.; Lanz, V. A.; Weingartner, E.; Baltensperger, U. Using aerosol light absorption measurements for the quantitative determination of wood burning and traffic emission contributions to particulate matter. *Environ. Sci. Technol.* **2008**, *42* (9), 3316−3323, DOI: 10.1021/es702253m.
(61) Schnaiter, M.; Horvath, H.; Mohler, O.; Naumann, K. H.; Saathoff, H.; Schock, O. W. UV-VIS-NIR spectral optical properties of soot and soot-containing aerosols. *J. Aerosol. Sci.* **2003**, *34* (10), 1421−1444, DOI: 10.1016/S0021-8502(03)00361-6.
(62) Schnaiter, M.; Schmid, O.; Petzold, A.; Fritzsche, L.; Klein, K. F.; Andreae, M. O.; Helas, G.; Thielmann, A.; Gimmler, M.; Mohler, O.; Linke, C.; Schurath, U. Measurement of wavelength-resolved light absorption by aerosols utilizing a UV-VIS extinction cell. *Aerosol. Sci. Technol.* **2005**, *39* (3), 249−260, DOI: 10.1080/027868290925958.
(63) Zhang, X. L.; Lin, Y. H.; Surratt, J. D.; Zotter, P.; Prevot, A. S. H.; Weber, R. J. Light-absorbing soluble organic aerosol in Los Angeles and Atlanta: A contrast in secondary organic aerosol. *Geophys. Res. Lett.* **2011**, *38*, DOI 10.1029/2011gl049385.